# Crime Art on the stone: graffiti vandalism on cultural heritage and the anti-graffiti role in its surfaces protection

Ombretta Cocco[1,*], Maura Carboni[2], Gianfranco Carcangiu[3],
Paola Meloni[4], Arianna Murru[1], Franca Persia[5] and Laura Solla[1]

[1] Università degli Studi di Cagliari, Dipartimento di Ingegneria Civile, Ambientale e Architettura (DICAAR), Via Marengo, 2, 09123 Cagliari, Italy
[2] Università degli Studi di Sassari, Dipartimento di Chimica e Farmacia, Via Vienna, 2, 07100 Sassari, Italy
[3] Istituto di Scienze dell'Atmosfera e del Clima (ISAC-CNR), UOS di Cagliari, c/o Università degli Studi di Cagliari, Dipartimento di Fisica, S.p. Monserrato-Sestu Km 0,70, 09042 Cagliari, Italy
[4] Università degli Studi di Cagliari, Dipartimento di Ingegneria Meccanica, Chimica e dei Materiali (DIMCM), Via Marengo, 2, 09123 Cagliari, Italy
[5] ENEA, Centro Ricerche Casaccia, Unità Tecnica Tecnologie dei Materiali, Via Anguillarese 301, 00123 Santa Maria di Galeria (Roma), Italy
*Corresponding author: *ombretta.cocco@unica.it*

## Abstract

Apparently perceived like an easy thing commonly used, spray paint is a very complex product composed by substances strongly penetrating particularly into the porous materials. This characteristic is very hazardous for our cultural heritage. The problem concerning the surfaces protection from paints and signs is very hard to solve, both for the difficulty to remove these substances and for the variety of the materials that react in a different manner to the various paints and cleaning treatments because of their different physical-chemical characteristics. With the aim to evaluate the damages originated by the spray paints on the stones and the efficacy of anti-graffiti products, some laboratory tests have been carried out. Two different limestones have been selected like supports: a little porous, polishable wakestone and a very porous bio-calcarenite with very scarce mechanical properties. Both these limestones are used as coverings and structural elements of buildings and monuments around Mediterranean basin. Concerning the spray paint cans, the most popular Montana mtn94 has been used, and two commercial anti-graffiti have been applied as protective products. Using Scanning Electron Microscope, Infrared Spectrometry, Colorimetry, Mercury Intrusion Porosimetry and Contact Angle Analysis the interactions stone-paint, stone-anti-graffiti and paint-anti-graffiti have been investigated. In order to evaluate the real efficacy of the anti-graffiti, some cleaning and removal paint tests have been carried out. The research

highlights that the anti-graffiti cause variations concerns the colour and/or the wettability in both limestones. Their effects are strictly related to the stonework and their microstructure but also the interaction with the paint is influent too.

*Key words*: anti-graffiti; protection; limestone.

### Introduction

The original aspect of our cities has been progressively modified by an uncontrolled diffusion of graffiti, which represents a real social emergency that often involved also our cultural heritage, when is a form of vandalism (Licchelli et al., 2011; Ciliberto et al., 2013). This generally prohibited expressive form, composed by coloured and large writings or signs that often overlap each other, is a real mass phenomenon observable from the suburbs to the historical centres of our cities. This form of expression can be realized using many coloured tools such as, for example, markers, varnishes and spray cans. Usually their specific chemical composition is unknown even if they are generally composed by organic or aqueous solvents, pigments and binders (Ciliberto et al., 2013). Spray paints can be divided in several categories depending on the nature of the resin composing them (i.e. thermoplastic resins such as acrylic, alkyd, silicon, nitrocellulose and polyurethane) (Zieba-Palus, 2003; 2005; Govaert and Magali, 2004; Buzzini et al., 2003; Buzzini and Massonnet, 2004). Colours performance (i.e. coverage, work speed, etc.) is strictly related to their composition and influenced by the viscosity and by the nature of the propellant. However, all of them are indelible and commonly used by graffiti-writers on the most different kind of supports. To contrast graffiti's phenomenon, many cleaning and protective methods were developed during the last decades. With reference to cleaning methods, they can be distinguished in two categories: physical-mechanical, which mainly

consist of air-powder abrasion, pressure washing, steam cleaning, sand blasting, laser technologies and other soft mechanical tools like lancets or brushes, and chemical, which include removers often based on organic solvents (AA. VV., 1999). The majority of these methods are now less used on cultural heritage's surfaces because of the possible damaging of their first layers (air-powder abrasion or sand blasting) or could allow the spreading and penetration in depth of the spray paints (solvents) (Goidanich et al., 2010). Regarding the protective methods, they consist of the application of a product called anti-graffiti (AG) on the stones surfaces. The anti-graffiti create a coating that avoids the spray paint penetration into the porous network of the material so that it can be easily removed. The protection of cultural surfaces through the use of a chemical coating able to provide a barrier against the penetration of the dye (spray or other graffiti tools) is a practice used in Unites States since 1960s (Carmona-Quiroga et al., 2010; Tarnowski et al., 2007). There are two types of anti-graffiti: the so called temporary (or sacrificial), which is removed during the cleaning process and need to be renewed, and the permanent, which can resist several cleaning cycles (Licchelli et al., 2011; AA.VV., 1999). Some authors also identify a third type, called semi-permanent, which can withstand two or three cleaning cycles (García and Malaga, 2012). Temporary anti-graffiti includes natural and/or microcrystalline waxes, polyacrylates, polysiloxanes or sugar-based polysaccharides while the permanent ones consist of compounds based on polyurethanes, polysiloxanes, polyacrylates, fluorinated

polymers and their combinations (Licchelli et al., 2011). As fundamental requirements, AG should have water and oil repellence and photo and chemical stability and a controlled rheology and glass transition temperature. In addition, they should not modify the original aspect of the surfaces on which they are applied, they should be environment-friendly and resistant to outdoor conditions (García and Malaga, 2012).

The possibility to apply protective coatings on cultural heritage surfaces has been tested on two different kinds of natural stones, very common in Sardinian monuments. With the aim to evaluate the damages originated by the spray paints on the selected stones and the efficacy of two commercial anti-graffiti locally produced, some laboratory and cleaning tests have been carried out.

### Experimental

*Materials and methods*

As supports two different limestones have been chosen because of their diffusion in all the Mediterranean basin like coverings and structural elements of buildings and monuments. The first one, called Biancone Tirreno (BT) from Orosei (Sardinia), is a very compact, polishable wakestone (Figure 1). The second one, locally called Pietra Cantone (PC), is a not polishable biomicritic limestone (Figure 2). Six untreated and not polished slabs of each stone (6 x 14 cm size) have been used in the experiments.

Concerning spray paints, two different colour (black and red) of Montana mtn94 spray paints, made by Montana Colors North America, Inc. have been chosen because of their popularity and diffusion among graffiti writers.

Regarding the anti-graffiti (AG), two commercial products have been selected because of their common use in protection of monuments. The first one, called AG1 is a sacrificial coating composed by paraffin waxes in water. This product, applied on a stone support, creates a protective coating easily removable using hot water. The second one, called AG2, is a semi-permanent anti-graffiti which, pursuant to its technical data sheet, should resist about 3-4 cleaning cycles. It is composed by two components. The first one as a primer, which contains an amino-functionalized polysiloxane water emulsion, while the second as a base, which contains an alkyl fluoride functionalized silane monomer + a lyophobic polymer. On porous stones it is necessary to firstly apply the primer and then the base while, for not porous
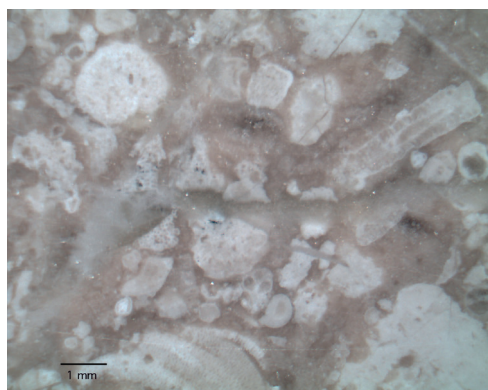


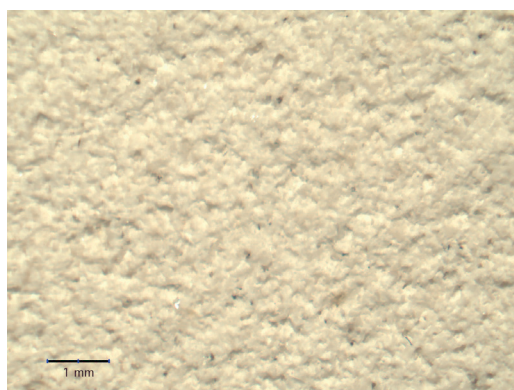Figure 1. Microphotograph of Biancone Tirreno (BT).



Figure 2. Microphotograph of Pietra Cantone (PC).

stones, it is sufficient only the application of the base, as suggested by technical data sheet of each product.

From the physical-mechanical point of view, limestones have been characterized following the UNI norms. Capillary absorption coefficient and imbibition coefficient have been measured respectively according to the UNI EN 15801:2010 and the UNI EN 13755:2008. Uniaxial compressive strength, flexural strength and elastic modulus have been measured by means of an oleo-dynamic press machine equipped by strain gauges (Fernando Belladonna 3305) respectively following the UNI EN 1926:2007, the UNI EN 13161:2008 and the UNI EN 14580:2005. Rupture energy has been determined according to UNI EN 14158:2005. Abrasion test (Amsler tribometer) has been carried out following the R.D. 16/11/39 n° 2234 art. 5. Apparent bulk density and real bulk density have been measured according to the UNI EN 1936:2007.

Microphotographs have been taken by means of a Motic DM143 Series Optical Microscopy. A Zeiss Optical Microscopy Axioscop 40 equipped with an AxioCam MRc5 and a Rigaku Miniflex II X-ray powder diffractometer operating with a CuKα monochromatic radiation at 15 kV-30 mA has allowed to highlight the mineralogical composition of the two limestones. TG-DTA analysis, carried out through a Netzsch STA 449 F3 Jupiter has allowed to establish their carbonates content. Their porosity has been measured through Mercury Intrusion Porosimetry (MIP) technique, performed on a Micromeritics Autopore IV 9500. SEM microscopy Zeiss Evo LS15 equipped with a LaB6 filament as electron source has been used to investigate stones microstructure before and after AG and paints treatments. The clarification of AG composition and the characterization of the binder of the spray paints have been performed through Fourier Transform Infrared Spectroscopy (FTIR), after application of these products on a glass sheet. A Thermo-Nicolet iN10 IR microscope has been used to collect the FTIR spectra in Attenuated Total Reflectance (ATR) mode with a Slide On Ge Micro Tip crystal ATR 350. The ATR-FTIR data have been processed with OMNIC software (Thermo Fisher Scientific Inc) and the experimental results have been compared with the spectral databases supplied with the same software.

Three slabs of each stone have been treated with AG1 and three with AG2. The same treatment has been repeated on some glass slides in order to avoid possible interferences due to the stones chemical composition. Both AG1 and AG2 have been applied twice through brush, following their respective technical data sheets. The second treatment has been applied only after the complete drying of the first one. In particular on each PC sample 3.50 g of AG1 and about 6 g of AG2 (4.74 g of primer and 1.24 g of base) have been altogether applied while on BT respectively 1.50 g and 0.74 g (only AG2 base). On PC, AG2 base has been applied twice only after one day, namely after the complete drying of the previous two treatments of AG2 primer. On BT has been applied twice only AG2 base, being BT a not porous stone. On each glass slides (2.5 x 7.5 cm size), respectively 31.2 mg of AG1, 37.0 mg of AG2 primer and 25.6 mg of AG2 base have been spread once by brush. All the samples have been aged for a week at room temperature and 60% RH. After the complete drying of the AG products on the stones only 0.92 g of AG1 and 0.26 g of AG2 (0.19 g of primer and 0.07 g of base) remained in PC as residual products while only 0.40 g of AG1 and 0.04 g of AG2 base in BT stones. As regards the glass slides, only 8.2 mg of AG1, 1.5 mg of AG2 primer and 1.4 mg of AG2 base remained as residual products. Then the slabs have been dirtied with the spray paints, both red and black. Before being applied, the cans which contained the spray paints have been shaken for 2 minutes in order to allow their different components to well mix together.

After placing the treated stone sample and the untreated glass slide at 20 cm far from each spray can, and trying to maintain a constant pressure on the spray nozzle, the sample has been dirtied with the paint for 5 seconds. All the slabs have been divided in three sections for each treatment: 1) only AG treatment; 2) AG treatment + red paint; 3) AG treatment + black paint. One slab for each treatment has been stored to be analysed through SEM. The other slabs have been subjected to some investigations and, finally, to cleaning tests. With the aim to evaluate how the surfaces have been changed after the application of AG and spray paints, SEM analysis have been carried out. In order to determine changes in hydrophobicity between the untreated and the treated surfaces, contact angle analysis have been carried out. The determination of the static contact angle has been evaluated through an apparatus in compliance with the norms in force (UNI EN 15802, 2010) building up 5 μl water drops onto the stones surface through a graduated micro-pipette. The images of the drops have been taken through a camera equipped with macro lens and analysed through the Low-Bond Axisymmetric Drop Shape Analysis (LBADSA) Plugin for ImageJ software (Stalder et al., 2006, 2010), which is based on the fitting of the Young-Laplace equation to the image data (Stalder et al., 2010). Mercury Intrusion Porosimetry (MIP) has been performed in order to evaluate porosimetric values of both untreated stones and changes after the application of both AG using six samples of PC for each treatment. On the contrary, with the aim to evaluate the chromatic variances generated by the anti-graffiti, colorimetric analysis have been carried out through a Minolta CM-525i Spectrophotometer, using a D65 illuminant, firstly on the untreated supports and at a later stage, after anti-graffiti application. The results have been reported in the CIEL*a*b* system, where L* represents brightness, while a* and b* colour parameters (a* on the red-green scale and b* on the yellow-blue scale). ΔE has

been evaluated according to the formula: $\Delta E = \sqrt{(\Delta L^*)2 + (\Delta a^*)2 + (\Delta b^*)2}$. The colorimetric measurements have been carried out only on PC, due to extreme variability in colour present in BT samples.

Cleaning tests have been carried out after one week ageing from the application of the spray paints, following the technical data sheets of AG used. The slabs protected with AG1 have been cleaned applying on their surfaces a piece of cotton-wool only soaked with hot water (about 55 °C). Being a sacrificial anti-graffiti, hot water should dissolve the waxes by which this AG is composed and as a consequence the paint. AG2 needs a cleaner product to perform the cleaning. The company suggests the use of a product based on dichloromethane. This product has been applied by brush, outdoor, wearing protective clothing. After the necessary curing time, dichloromethane should remove the spray paint keeping intact the protective underlying layers for at least three cleaning cycles. SEM and FTIR analysis have been also carried out in order to evaluate the results of cleaning tests.

## Result and discussion

### Characterization of the materials

Table 1 shows some of the most relevant physical and mechanical properties of investigated stones. XRD analysis has identified calcite as exclusive mineralogical phase both in Biancone Tirreno (BT) and in Pietra Cantone (PC). In addition rare allochemical clasts (such as quartz, feldspar and phyllosilicate) have been detected in PC. MIP analysis has revealed a very low porosity (about 1-2%) in BT and high porosity (between 32.5-39.5%) in PC.

In Figures 3 and 4 SEM images respectively of BT and PC are depicted. BT exhibits a very compact structure while PC shows a typical biomicritic fabric.

In order to support the evaluation of paints binder chemical composition, FTIR spectra of

Table 1. Physical and mechanical properties of BT and PC.

| PHYSICAL AND MECHANICAL PROPERTIES | BT | PC |
|---|---|---|
| Total porosity (MIP) (%) | 1.5 ± 0.5 | 36.0 ± 3.5 |
| Capillary absorption coefficient (g/cm2) | 0.0012 ± 0.0014 | 0.015 ± 0.0015 |
| Imbibition coefficient (%) | 0.8 ± 0.042 | 15.0 ± 6.5 |
| Uniaxial compressive strength (MPa) | 120 ± 15 | 12 ± 2 |
| Flexural strength (MPa) | 16.5 ± 2.5 | 2.3 ± 0.7 |
| Elastic modulus (GPa) | 61.0 ± 1.5 | 0.6 ± 0.1 |
| Rupture energy (J) | 5.0 ± 0.5 | 1.5 ± 0.3 |
| Abrasion test (mm) | 37 ± 1.8 | 4.5 ± 0.3 |
| Apparent bulk density (g/cm3) | 2.63 ± 0.35 | 1.60 ± 0.30 |
| Real bulk density (g/cm3) | 2.70 ± 0.2 | 2.65 ± 0.3 |
| Carbonates (%) | 96.7 ± 2 | 87.2 ± 3 |
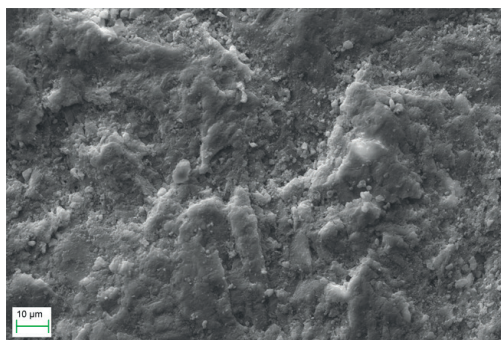


Figure 3. SEM image of BT (2000 X - SE1).
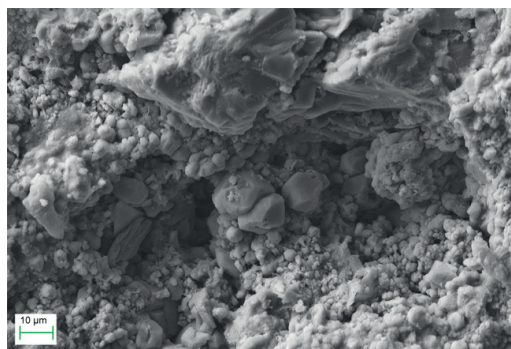


Figure 4. SEM image of PC (2000 X - SE1).

both paints (red and black) sprayed onto the glass support are reported in Figures 5a (red) and 5b (black). Both FTIR profiles are different from each other because belong to two different paint colours which are characterised by the same binder. Both of them match the standard reference spectrum of a binder ascribable to an alkyd resin (Figure 5c), recognizable for the presence of some peaks, particularly at 2925 and 2858 cm$^{-1}$ (due to C–H stretching of the aliphatic chains), at 1730 cm$^{-1}$ (related to C=O stretching of the ester carbonyl group), at 1270 cm$^{-1}$ (referred to C–H bending bands), at 1122 and 1070 cm$^{-1}$ (due to C–O bending), and at 746 and 710 cm$^{-1}$ (due to C–H torsion bands). Alkyds work as binders and film-forming agents in the used paints.

Concerning AG1 applied on a glass slide in order to avoid possible interferences due to the stones chemical composition, very strong peaks appear in the range of 2840-2920 cm$^{-1}$, due to the stretching vibrations of aliphatic chains, typical of synthetic polymer waxes (Derrick et al., 1999; Silverstein et al., 1991). Confirmatory
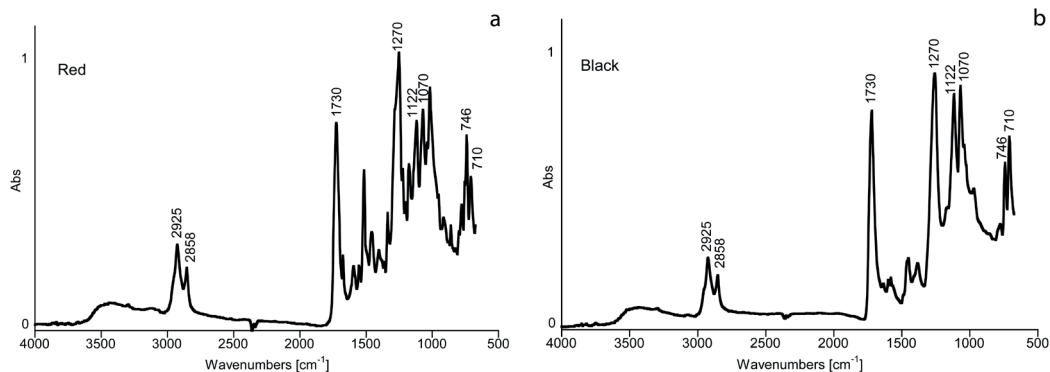
Figure 5 a,b. ATR-FTIR spectra of the varnishes sprayed on a glass slide: (a) red; (b): black.
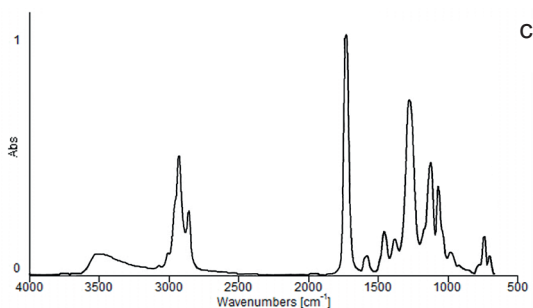


Figure 5c. Reference spectrum of an alkyd resin (Hummel Polymer Sample Library).

bands for waxes are the small and sharp doublets at 730/722 cm$^{-1}$. An additional strong and sharp peak, located at 1107 cm$^{-1}$, could be related to the presence of C–O–C groups in the polymer structure (Silverstein et al., 1991). The ATR-FTIR spectra of AG1 applied on both stones almost match those obtained by the analysis of AG1 applied on a glass slide. They could be differentiate by the additional presence of one and very weak signal at 1396 cm$^{-1}$ on BT stone spectrum, and more intense signals at 1403 and 875 cm$^{-1}$ on PC stone spectrum. All these signals are ascribed to calcite. Differences in roughness of the two calcareous stones as well as the presence of a polymer coating characterized by a variable thickness on the stones surface could explain this result. The ATR-FTIR spectra of

AG1, both spread on a glass slide and on the stones, are respectively depicted in Figure 6a and in Figure 6b.

Figure 6c shows the standard spectra referred to untreated stones, which highlights the presence of a weak absorption peak at around 1000 cm$^{-1}$, more evident on PC stone spectrum. A similar peak appears on PC treated both with AG1 and AG2, and on the glass slides treated with AG2. Regarding AG1 on PC stone this peak, not visible on treated glass slide, could be ascribable to the Si phases naturally present in that kind of bio-calcarenite. On the other hand, AG2 shows a peak at around 1000 cm$^{-1}$ ascribable to the presence of Si-O groups characterising this product. This is visible on the glass slide as well on PC stone, where overlaps
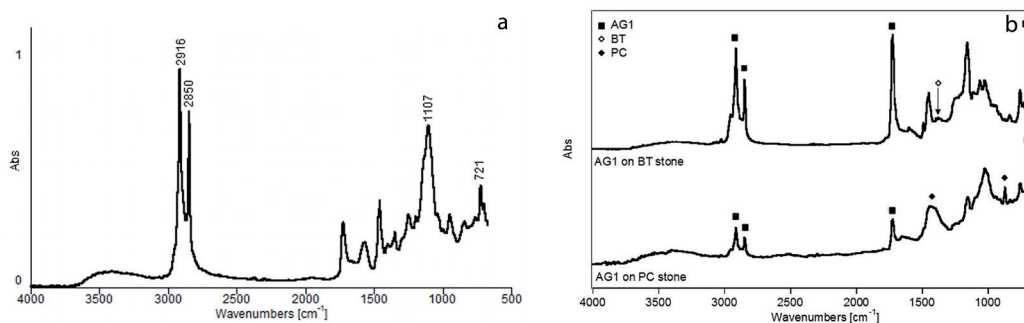
Figure 6 a,b. ATR-FTIR spectrum of AG1 coating applied: (a) on a glass slide; (b) on the stones.
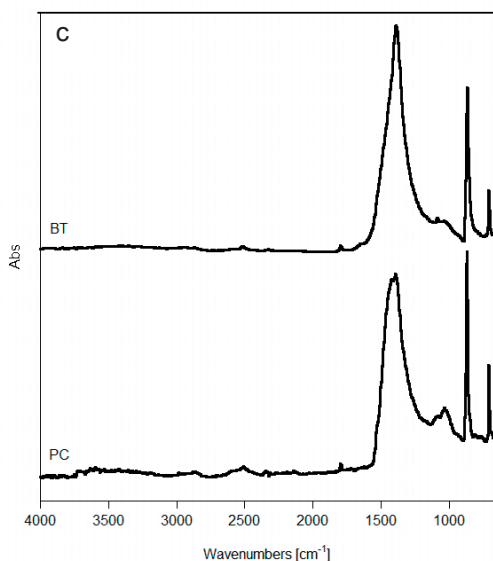


Figure 6c. ATR-FTIR reference spectrum of untreated BT and PC stones.

chemical composition. AG2 primer spectrum (Figure 7a) shows strong absorptions in the range of 830-1110 cm$^{-1}$, due to the stretching vibrations of Si-O bands, moreover, an additional low absorption peak occurs at 2963 cm$^{-1}$, due to the vibrations of aliphatic chains (Derrick et al., 1999). In AG2 base (Figure 7b), dominant IR bands in the range of 1000–1300 cm$^{-1}$ arise from the different deformation modes of C-F bonds (Silverstein et al., 1991; Yang et al., 2006), while the peak at 1736 cm$^{-1}$ is due to the acrylic component (Silverstein et al., 1991). However, both compounds exhibit well different profiles in the fingerprint region (between 650 and 1800 cm$^{-1}$).

AG2 primer (AG2p) applied on PC samples is recognised through bands at 1008 and 798 cm$^{-1}$. AG2 base (AG2b) is easily identified both on BT and on PC stones through the detection of peaks at 1736, 1200 and 1146 cm$^{-1}$, even if on PC they decrease because of the presence of the additional AG2p layer. However, the bands related to calcite (1396, 871 and 713 cm$^{-1}$) are the strongest signals.

Finally, the paints have been applied on untreated BT and PC, and treated ones with anti-graffiti (AG1 and AG2). All the spectroscopic analysis carried out on stained samples, have revealed that the paints cover the signals of the underlying surface.

the Si signal naturally present in that kind of bio-calcarenite.

Regarding to AG2 treatment, either the primer or the base, have been firstly analysed separately spread on the glass slides in order to avoid possible interferences due to the stones
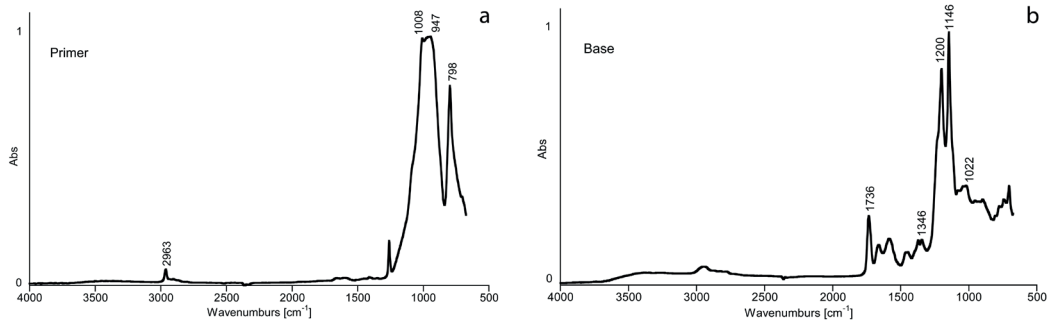
Figure 7. ATR-FTIR spectra of AG2 coatings obtained by casting on a glass slide: (a) primer; (b) base.
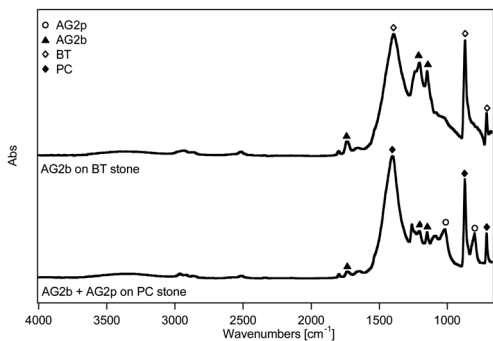


Figure 8. ATR-FTIR spectra of the stones surfaces protected with AG2 anti-graffiti system (b = base; p = primer).
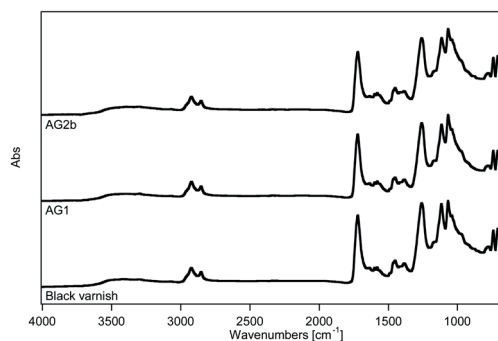


Figure 9. ATR-FTIR spectra of the BT stone surfaces sprayed with the black varnish.

In Figure 9, the ATR-FTIR spectra acquired on the varnished BT samples are reported as an example. In all the samples, the peaks at 1728, 1452 and 1146 cm$^{-1}$, related to the paint coating, are strongly dominant and only detected on the stained surfaces.

FTIR analysis on three months natural aged samples showed results totally coincident with those obtained during the first stage of analysis.

*Morphological analysis on treated stones*

In Figure 10a and 11a are respectively presented SEM images of BT and PC after the application of AG1: it is possible to notice the presence of a very thin coating on both stones.

AG1 give to the surface of both stones an almost covering effect, characterized by areas in which AG1 seems not to be completely adherent to the support below, creating bubbles and craquelures, especially on PC. A similar result is obtained through SEM observation of BT treated with AG2: the anti-graffiti creates an irregular protective thin coating that allows to glimpse stones morphology (Figure 10b). Different behaviour is shown by the bi-component AG2 applied on PC. It forms a microcracked coating that seems to be very adherent to the stones surface (Figure 11b). This effect could be related to the application of the additional primer layer.
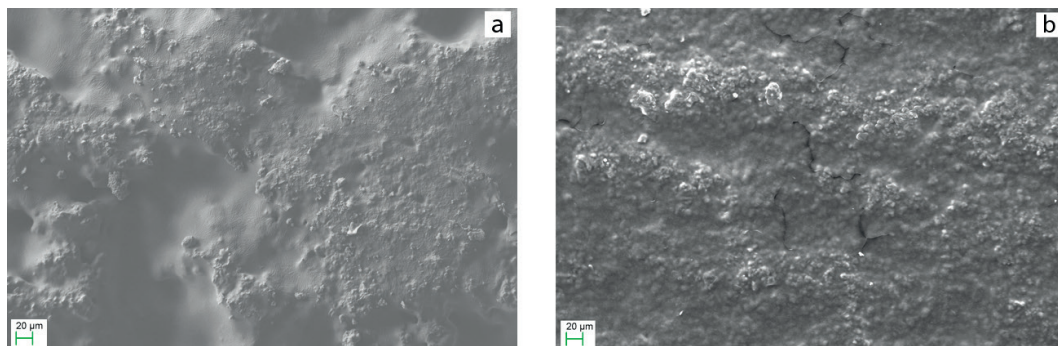
Figure 10. SEM image of BT (500 X - SE1) treated: (a) with AG1; (b) with AG2 (base).
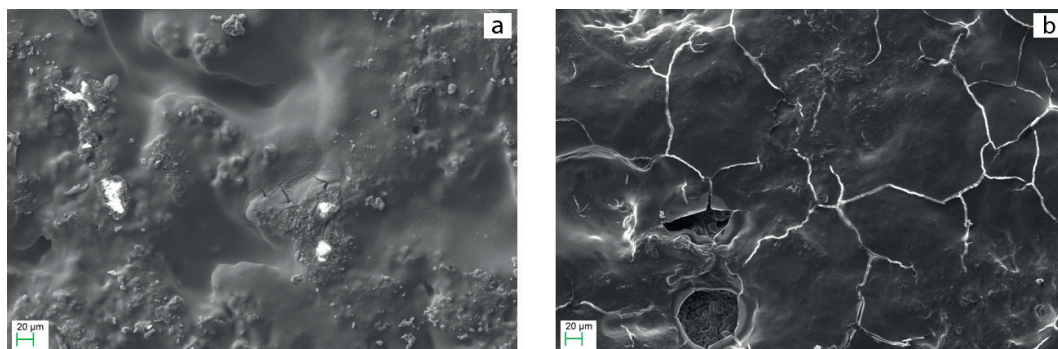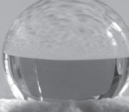


Figure 11. SEM image of PC (500 X - SE1) treated: (a) with AG1; (b) with AG2 (primer + base).

Table 2. Contact angle data and drops images.

| | UNTREATED | | TREATED WITH AG1 | | TREATED WITH AG2 | |
|---|---|---|---|---|---|---|
| BT | 25.549° | | 91.384° | | 120.575° | |
| PC | - | - | 96.138° | | 140.743° | |

*Contact angle analysis*

Contact angle analysis (Table 2) shows how the wettability of the materials completely changes on both AG treated limestones, exhibiting hydrophobic properties (García and Malaga, 2012). These changes are highlighted especially on PC treated with primer + baseAG2, that probably forms a protective thicker coating. In addition, the higher contact angle recorded for AG2 treatment is probably due to the presence of fluorine that has surely a high hydrophobicity (Ruffolo et al., 2010). Contact angle measures on untreated PC have not been performed because of its roughness and open porosity.

*Porosimetric analysis*

In Table 3 are reported the porosimetric data that show how the porosity of treated samples slightly decrease. Cumulative intrusion data reveal a delay in the penetration of mercury, presumably due to the presence of the AG coatings that do not allow the Hg to intrude using a pressure similar to that of the untreated sample. Therefore Hg presumably starts to intrude through the micro-cracks visible in the SEM image. This effect is more evident on the samples treated with AG1 (Figure 12). Analysing the porous structure, therefore it is not significantly altered. This is a crucial

Table 3. A comparison between the porosity of PC: untreated, treated with AG1 and treated with AG2.

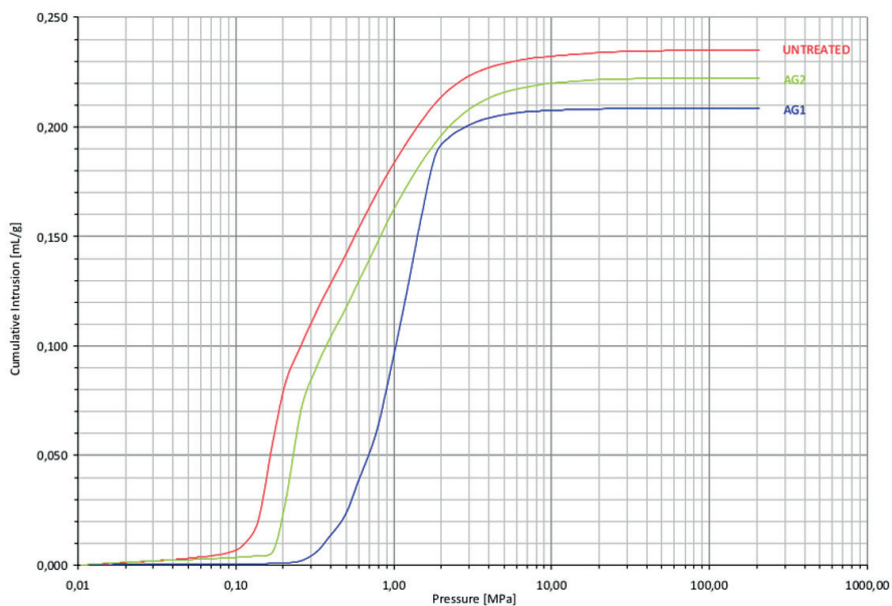|  | UNTREATED | AG1 | AG2 |
| --- | --- | --- | --- |
| MIP ANALYSIS | 36.0 (±3.5) | 34.5 (±3.0) | 34.2 (±3.5) |



Figure 12. The curves trend (cumulative intrusion/pressure) of PC untreated, treated with AG1 and treated with AG2.

Table 4. Colorimetric data of PC treated with AG1.

|        | NT              | AG1              |
|--------|-----------------|------------------|
| L*     | 88.77 (± 0.03)  | 86.46 (± 0.10)   |
| a*     | 0.44 (± 0.05)   | 0.51 (± 0.01)    |
| b*     | 9.56 (± 0.19)   | 13.86 (± 0.06)   |
| ΔL*    | - 2.31          |                  |
| Δa*    | 0.07            |                  |
| Δb*    | 4.24            |                  |
| ΔE     | 4.83            |                  |

Table 5. Colorimetric data of PC treated with AG2.

|        | NT              | AG2              |
|--------|-----------------|------------------|
| L*     | 87.91 (± 0.16)  | 86.94 (± 0.12)   |
| a*     | 0.59 (± 0.07)   | 0.53 (± 0.02)    |
| b*     | 9.66 (± 0.11)   | 11.25 (± 0.05)   |
| ΔL*    | - 0.97          |                  |
| Δa*    | - 0.06          |                  |
| Δb*    | 1.59            |                  |
| ΔE     | 1.86            |                  |

point for a good conservation condition for the substrate (La Russa et al., 2011; Belfiore et al., 2012). Due to the very low porosity of BT, porosimetric analysis has been carried out only on PC samples.

*Colorimetric analysis*

In Tables 4 and 5 are shown the results of colorimetric investigations. The most relevant variation is detected in b* for both samples (up to 4.24 for AG1) meaning that the coating application turns yellow. The value of ΔE (total colour difference) is 4.83 for AG1 (Table 4) and 1.86 for AG2 (Table 5). These variations are almost acceptable for AG1 and considered minimal for AG2 (García and Malaga, 2012; Palazzi, 1995). In the field of cultural heritage it is considered acceptable a variation value below 5 for treated materials compared to untreated ones (Ruffolo et al., 2014). The colorimetric measurements have been carried out only on PC, because of the extreme variability in colour present on BT samples.

*Application of spray paints and evaluation of cleaning tests*

The application of both black and red spray paints above a layer of AG1 shows the development of a rough-wavy covering coating
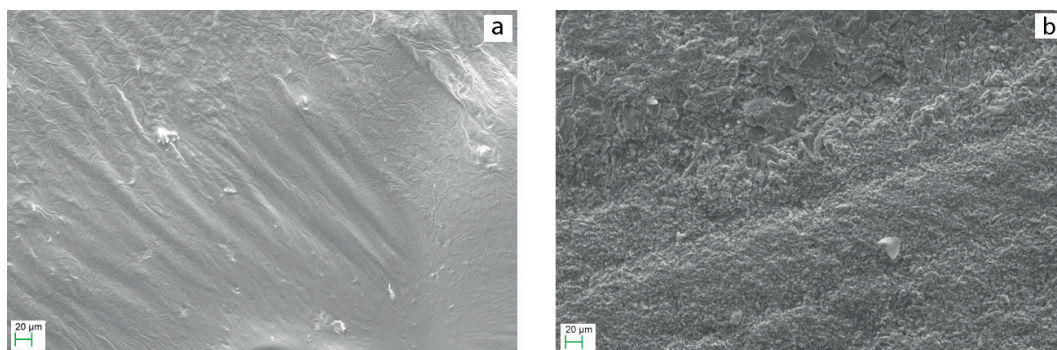
Figure 13. SEM image of BT (500 X – SE1) treated with AG1: (a) dirtied with black varnish; (b) dirtied with black varnish and cleaned with hot water.
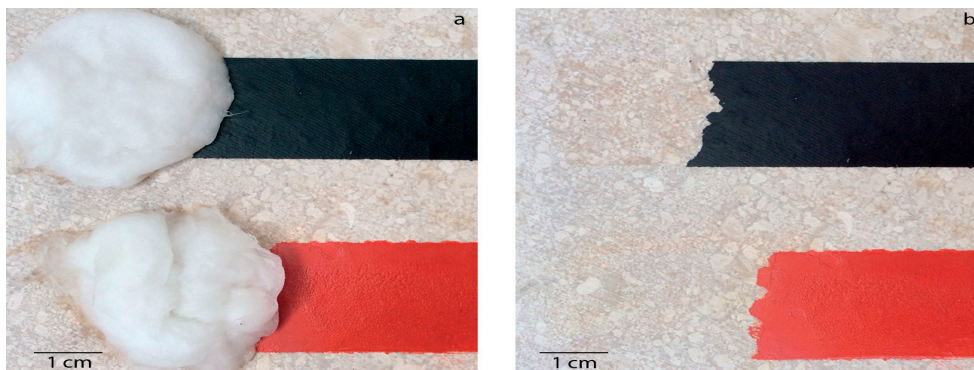
Figure 14. Visible image of the first cleaning cycle on BT treated with AG1 and dirtied with red and black varnishes: (a) the application of a piece of cotton wool soaked with hot water; (b) the result of the first cleaning cycle.

on BT support. Through SEM observation, this coating appears partially swollen, as if it is not completely anchored to the underlying layer (Figure 13a).

Cleaning test showed how applying hot water through a piece of cotton-wool (Figure 14a), varnish is completely removed (Figure 14b).

Further SEM observations (Figure 13b) on cleaned BT confirm that almost all AG1 layer is removed through cleaning procedure. In addition, ATR-FTIR spectrum of cleaned BT is compared with those of untreated BT. They perfectly match, showing only the characteristic signals of calcite.

On the other hand, both black and red vanishes applied on BT protected with AG2 create a compact and adherent layer that still permitted to see stone morphology (Figure 15a). Applying the cleaner product composed by dichloromethane (Figure 16a), the paint is completely removed from BT as demonstrate by Figure 16b. ATR-FTIR analysis confirm the complete removal of both spray paints and the permanence of AG2 observable by the presence of strong and sharp peaks at 1736, 1200 and 1146 $cm^{-1}$. Regarding the durability of AG2 treatment, SEM investigations reveal that the coating uniformity
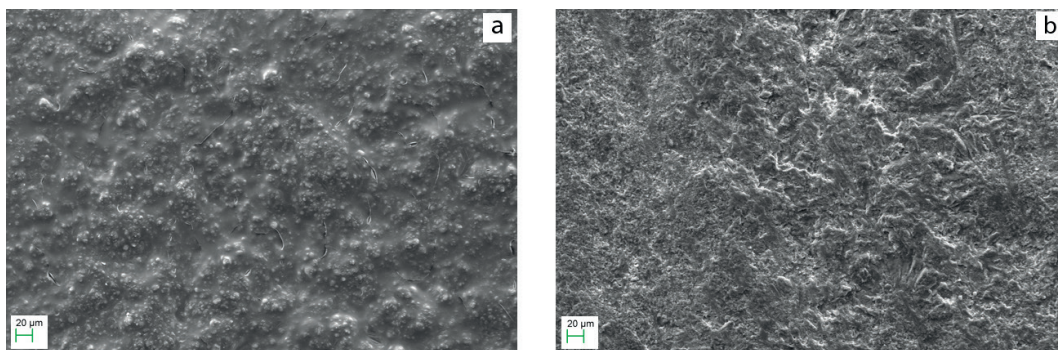


Figure 15. SEM image of BT (500 X – SE1) treated with AG2 (base): (a) dirtied with black varnish; (b) dirtied with black varnish and cleaned with dichloromethane.
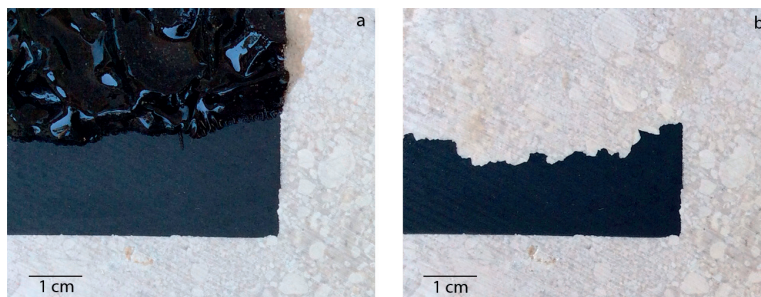
Figure 16. Visible image of the first cleaning cycle on BT treated with AG2 (base) and dirtied with black varnish: (a) the application of dichloromethane; (b) the result of the first cleaning cycle.
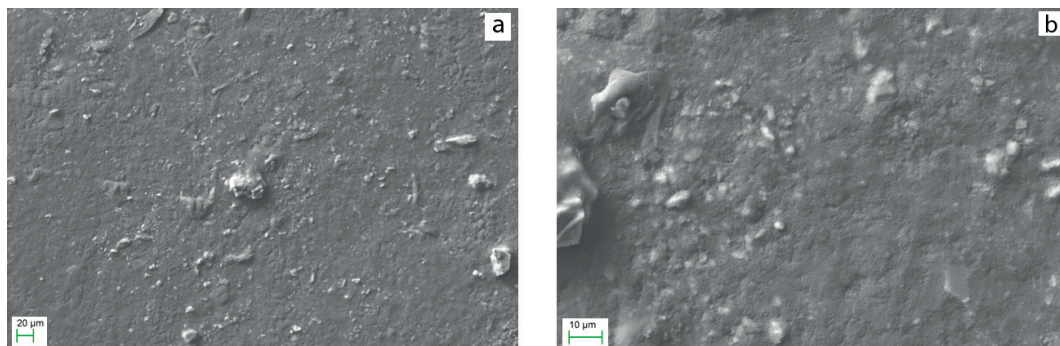


Figure 17. SEM image of PC treated with AG1: (a) dirtied with black varnish (500 X – SE1); (b) dirtied with black varnish and cleaned with hot water (2000 X – SE1).
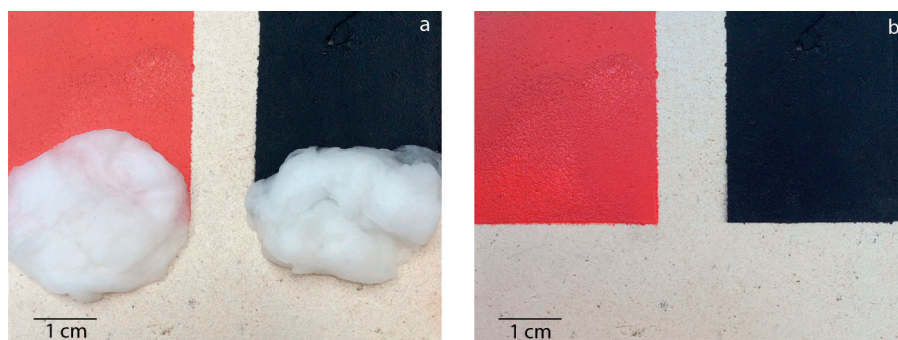


Figure 18. Visible image of the first cleaning cycle on PC treated with AG1 and dirtied with red and black varnishes: (a) the application of a piece of cotton wool soaked with hot water; (b) the result of the first cleaning cycle.

is compromised after the second cleaning cycle and some little paint traces are still visible on BT sample (Figure 15b).

A compact coating almost flat and fairly regular (Figure 17a) is detected on treated PC stone (AG1 + varnishes).

The application of hot water with a piece of cotton-wool (Figure 18a) does not allow to remove neither the varnish nor AG1; both remain strongly joined to the underlying PC surface (Figure 18b).

SEM investigation (Figure 17b) and FTIR analysis confirm these data.

SEM observations on PC treated with AG2+varnishes highlight the presence of some bubbles and a quite adherent and irregular film that covers the surface (Figure 19a). Analyzing PC support after dichloromethane cleaning (Figure 20a), varnish is still visible (Figure 20b). ATR-FTIR analyses highlight signals of residual paints + AG2 in some areas whereas in others only the characteristic peaks of calcite. This is also observed by SEM, where AG2 + varnished portions are still notable in some areas while in others appears again stone morphology (Figure 19b).
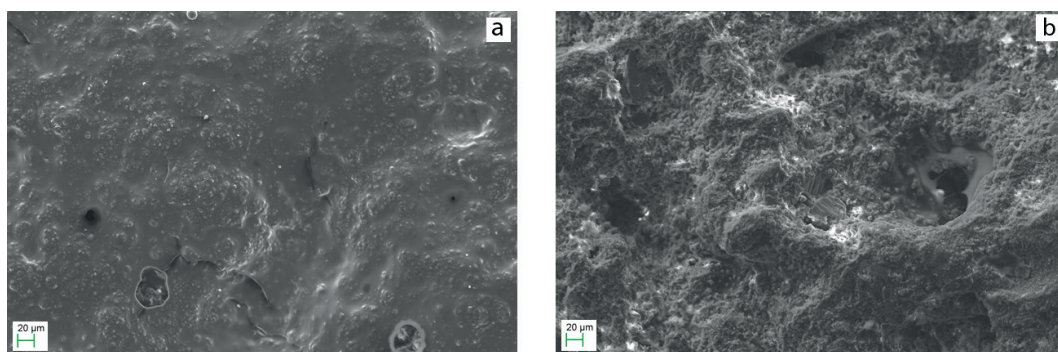


Figure 19. SEM image of PC (500 X – SE1) treated with AG2 (primer + base) - (a) dirtied with black varnish; (b) dirtied with black varnish and cleaned with dichloromethane.
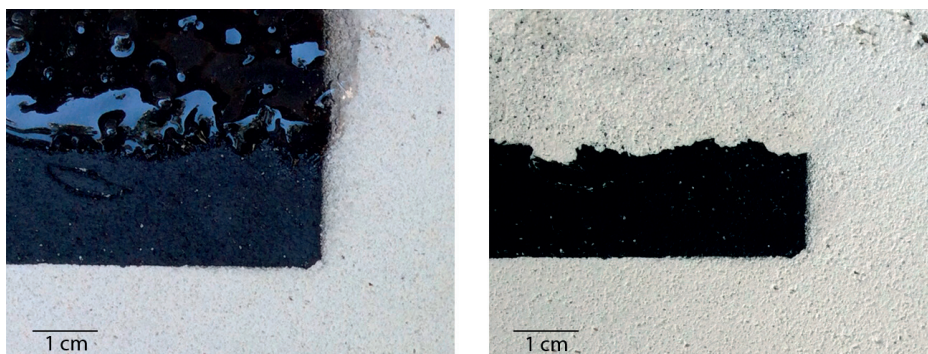


Figure 20. Visible image of the first cleaning cycle on PC treated with AG2 and dirtied with black varnish - (a) the application of dichloromethane; (b) the result of the first cleaning cycle.

## Conclusions

The results obtained in this research have highlighted the different behaviour and the effectiveness of two commercial anti-graffiti, one sacrificial (AG1) and one semi-permanent (AG2), applied on different microstructured limestones. The most relevant parameter was found to be the limestone fabric, therefore the specific surface, the porosity and the roughness. These parameters influence the adhesion capability of both anti-graffiti, so their protective effects. Both AG1 and AG2 exhibit good performances on not porous stones, preventing the penetration of the varnishes and allowing the easy cleaning if dirtied. Another property that influences the behaviour of these AG is the related hydrophobicity measured by static contact angle. All the measured values are higher than 90°, considered the minimum static contact angle to confer sufficient hydrophobicity to a surface (García and Malaga, 2012). Therefore the application of both AG strongly modifies the surfaces of both stones developing good water repellence properties and, consequently, completely decreasing their wettability. Colorimetric measurements have been crucial to evaluate if the aesthetic appearance of the stones changed from the chromatic point of view. The colorimetric difference ΔE between untreated and treated stones should be < 5 not to be perceivable by human eye (García and Malaga, 2012) and so suitable for the surfaces of Cultural Heritage. Both AG tested respect this requirement. Finally, cleaning tests have been carried out in order to evaluate the effectiveness and the durability of the AG studied. As confirmed also by FTIR analysis and SEM observations, they result effective on not porous stones while they are still unsuitable for the porous ones.

This work underlines the difficulties in evaluating the real effectiveness of AG treatments because their performances are strictly dependent on the microstructural features of the stones and on their finishing. These natural and artificial limestone features greatly influence the coating adhesion and the spreading of varnishes into the stone matrix. All these parameters need to be considered even if the chemical composition of the stone is similar. In fact, in spite of the fact that both materials used as supports were limestones, for very porous stones the protective efficiency have been almost scarce, consequently, an easier penetration of the varnishes into the porous network has been observed. Finally, concerning the semi-permanent anti-graffiti (AG2) durability, that according to the technical data sheet should resist about three-four cleaning cycles with dichlorometane, experimental data have revealed that only one cycle is able to partially compromise the AG coating on the investigated matrix, leaving the stone vulnerable to the graffiti paints.

## Acknowledgements

# References

AA.VV. (1999) - Graffiti on historic buildings and monuments - Methods of removal and prevention - Technical advice note, English Heritage, London.

Belfiore C.M., Fichera G.V., La Russa M.F. and Pezzino A. (2012) - The Baroque architecture of Scicli (south-eastern Sicily): characterization of degradation materials and testing of protective products. *Periodico di Mineralogia*, 81(1), 19-33.

Buzzini P. and Massonnet G. (2004) - A market study of green spray paints by Fourier transform infrared (FTIR) and Raman spectroscopy. *Science & Justice*, 44(3), 123-131.

Buzzini P., Massonnet G. and Mizrahi S. (2003) - Analysis of green spray paints: population study and its application in a forensic casework, 136 Forensic Science International, Suppl 1, 355.

Carmona-Quiroga P.M., Martínez-Ramírez S., Sánchez-Cortés S., Oujja, Castillejo M. and Blanco-Varela M.T. (2010) - Effectiveness of antigraffiti treatments in connection with penetration depth determined by different techniques. *Journal of Cultural Heritage*, 11, 297-303.

Ciliberto E., Battaglia D.M., Capello C., Gatto M., La Delfa S., Masieri M. and Quarta G. (2013) - Graphic Vandalism: study of the interaction of spray varnishes with stone materials and test of some antigraffiti treatments. *Procedia Chemistry*, 8, 165-174.

Derrick M.R., Stulik D.C. and Landry J.M. (1999) - Infrared Spectroscopy in Conservation Science, The Getty Conservation Institute, Los Angeles.

García O. and Malaga K. (2012) - Definition of the procedure to determine the suitability and durability of an anti-graffiti product for application on cultural heritage porous materials. *Journal of Cultural Heritage*, 13, 77-82.

Goidanich S., Toniolo L., Jafarzadeh S. and Odnevall Wallinder I. (2010) - Effects of wax-based anti-graffiti on copper patina composition and dissolution during four years of outdoor urban exposure. *Journal of Cultural Heritage*, 11, 288-296.

Govaert F. and Magali B. (2004) - Discriminating red spray paints by optical microscopy, Fourier transform infrared spectroscopy and X-ray fluorescence. *Forensic Science International*, 140(1), 61-70.

La Russa M.F., Barone G., Belfiore C.M., Mazzoleni P. and Pezzino A. (2011) - Application of protective products to ''Noto'' calcarenite (south-eastern Sicily): a case study for the conservation of stone materials. *Environmental Earth Sciences*, 62(6), 1263-1272.

Licchelli M., Marzolla S.J., Poggi A. and Zanchi C. (2011) - Crosslinked fluorinated polyurethanes for the protection of stone surfaces from graffiti. *Journal of Cultural Heritage*, 12, 34-43.

Palazzi S. (1995) - Colorimetria. La scienza del colore nell'arte e nella tecnica, Firenze.

R.D. (1939) - Regio Decreto del 16/11/39 n° 2234 articolo n° 5.

Ruffolo S.A., La Russa M.F., Malagodi M., Oliviero Rossi C., Palermo A.M. and Crisci G.M. (2010) - ZnO and $ZnTiO_3$ nanopowders for antimicrobial stone coating. *Applied Physics A, Materials Science & Processing*, 100, 829-834.

Ruffolo S.A., La Russa M.F., Aloise P., Belfiore C.M., Macchia A., Pezzino A. and Crisci G.M. (2014) - Efficacy of nanolime in restoration procedures of salt weathered limestone rock. *Applied Physics A, Materials Science & Processing*, 114, 753-758.

Silverstein R.M., Bassler G.C. and Morill T.C. (1991) - Spectrometric Identification of Organic Compounds, 5th edition, John Wiley & Sons, New York, 91-164.

Stalder A.F., Kulik G., Sage D., Barbieri L. and Hoffmann P. (2006) - A Snake-Based Approach to Accurate Determination of Both Contact Points and Contact Angles. *Colloids And Surfaces A: Physicochemical and Engineering Aspects*, 286(1-3), 92-103.

Stalder A.F., Melchior T., Müller M., Sage D., Blu T. and Unser M. (2010) - Low-Bond Axisymmetric Drop Shape Analysis for Surface Tension and Contact Angle Measurements of Sessile Drop. *Colloids and Surfaces A: Physicochemical and Engineering Aspects*, 364(1-3), 72-81.

Tarnowski A., Zhang X., McNamara C., Martin S.T. and Mitchell R. (2007) - Biodeterioration and Performance of Anti-graffiti Coatings on Sandstone and Marble. *Journal of Canadian Association for Conservation*, 32, 3-16.

UNI EN 15802 (2010) - Conservation of cultural property. Test methods. Determination of static contact angle.

UNI EN 13755 (2008) - Natural stone test methods. Determination of water absorption at atmospheric pressure.

UNI EN 15801 (2010) - Conservation of cultural property. Test methods. Determination of water absorption by capillarity.

UNI EN 1926 (2007) - Natural stone test methods. Determination of uniaxial compressive strength.

UNI EN 13161 (2008) - Natural stone test methods. Determination of flexural strength under constant moment.

UNI EN 14580 (2005) - Natural stone test methods. Determination of static elastic modulus.

UNI EN 14158 (2005) - Natural stone test methods. Determination of rupture energy.

UNI EN 1936 (2007) - Natural stone test methods. Determination of real density and apparent density, and of total and open porosity.

Yang T., Yao L., Peng H., Cheng S. and Park I.J. (2006) - Characterization of a low-wettable surface based on perfluoroalkyl acrylate copolymers. *Journal of Fluorine Chemistry*, 127, 1105-1110.

Zieba-Palus J. (2003) - Application of FTIR in Examination of Spray Paints on the Wall, 136 Forensic Science International, Suppl 1, 358.

Zieba-Palus J. (2005) - Examination spray paints by the use of reflection technique of microinfrared spectroscopy. *Journal of Molecular Structure*, 744-747, 229-234.